Cement & Concrete Composites 33 (2011) 725–734

Contents lists available at ScienceDirect

Cement & Concrete Composites

journal homepage: www.elsevier.com/locate/cemconcomp

Permeation of water and gases through cracked textile reinforced concrete

Viktor Mechtcherine *, Matthias Lieboldt

Institute of Construction Materials, Faculty of Civil Engineering, Technische Universität Dresden, Dresden, Germany

ARTICLE INFO

Article history:
Received 14 October 2010
Received in revised form 4 April 2011
Accepted 5 April 2011
Available online 12 April 2011

Keywords:
Textile-reinforced concrete
Multiple cracking
Water absorption
Permeability
Self-healing

ABSTRACT

Textile reinforced concrete (TRC) is a high-performance, cement-based composite consisting of fine-grained concrete and textile reinforcement, the latter usually consisting of glass or carbon multi-filament yarns. When subjected to tensile loading, TRC shows pronounced strain hardening behaviour accompanied by multiple cracking. The superior mechanical performance of TRC can be used very efficiently in the strengthening and repair of structural elements made of reinforced concrete or other traditional materials. The durability of restored structures with such TRC layers depends directly on the resistance of TRC to the transport of fluids and gases into and through the repair material. In this experimental study the effects of multiple cracking on the permeation of water and gases through TRC are investigated.

For permeability testing special equipment was developed to facilitate in situ measurement of the water and gas transport properties of cracked TRC at chosen strain levels under uniaxial tensile loading. Further parameters of the study were the fineness and coating of the yarns comprising the textile reinforcement. In the case of uncoated textile, an increase in the fineness of the yarns as well as the residual strain led to a considerable increase in water absorption. The permeation of oxygen and water through cracked TRC correlated with the induced strain and the crack characteristics, i.e. the number of cracks and crack width. The crack pattern itself depended on the choice of the particular textile reinforcement. The influence of imposed strain on the permeation of water in cracked TRC was described by a simple model based on Hagen–Poiseuille's Law. Furthermore, the effect of self-healing phenomena on the transport properties of TRC was investigated. The self-healing of fine cracks led to a very pronounced reduction in the transport rates over time.

1. Introduction

1.1. Applications of textile reinforced concrete

The major characteristic features of textile reinforced concrete (TRC) are its pronounced pseudo-ductile behaviour and high tensile strength. This material's excellent mechanical properties offer great possibilities with respect to its application in new construction as well as in the strengthening and repair of structural elements made of reinforced concrete or other traditional materials. The textile reinforcement, when positioned near the concrete surface, makes for good crack distribution and very effective crack bridging, leading to very narrow crack widths. The advantage of alkali-resistant (AR) glass or carbon fibres in comparison with steel reinforcement is that they are not susceptible to corrosion. In contrast to steel reinforcements, a concrete covering is not necessary. Therefore, slimmer and lighter construction elements and thinner reinforcement layers can be produced.

A practical application for the strengthening of existing structures using textile reinforced concrete was carried out in 2006 for retrofitting of an RC roof shell at the University of Applied Sciences in Schweinfurt, Germany. The project was carried out with the technical support of the Collaborative Research Centre SFB 528 "Textile Reinforcement for Structural Strengthening and Retrofitting" of the TU Dresden. The 80 mm thick RC hypar-shell has a side length of approximately 27 m and a maximum span of approximately 39 m, cf. Fig. 1. Large deformations (up to 200 mm drop) in the shell's cantilevered wings had been measured; the design tensile stress levels in the upper steel reinforcement layer of the shell had been exceeded significantly, such that strengthening measures were absolutely necessary. A TRC layer of 15 mm thickness containing three layers of textile sheets made of carbon fibre was applied to these particular areas in order to increase the load carrying capacity and to prevent further increase in deformations [1].

Schladitz et al. [2] give another example of structural strengthening using TRC. This case concerns an historical school of engineering in Zwickau, Germany, built in 1903 and restored during the last two years to serve in the future as home to the city tax authority. One part of this school has a large, barrel-shaped concrete roof which covers a room measuring 16 m × 7 m. The roof consists of curved steel-reinforced concrete slabs of 80 mm thickness, which are supported by eleven beams with a width of 200 mm and a height of 250 mm. The beams were strengthened

* Corresponding author.
E-mail address: mechtcherine@tu-dresden.de (V. Mechtcherine).

0958-9465/$ - see front matter © 2011 Elsevier Ltd. All rights reserved.
doi:10.1016/j.cemconcomp.2011.04.001

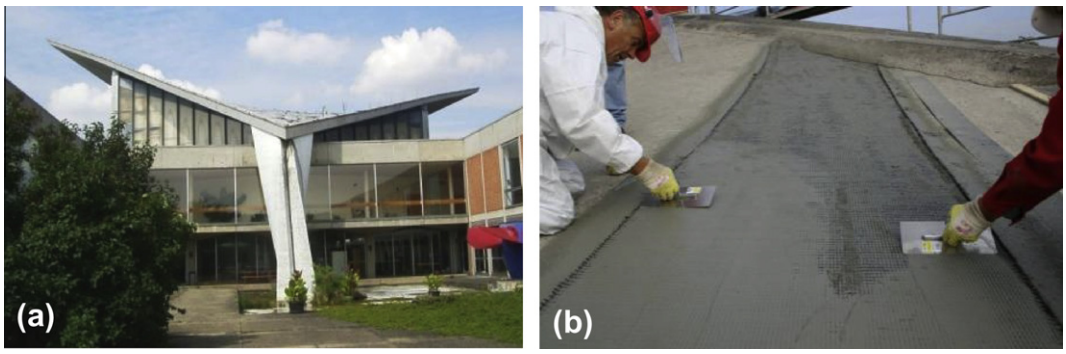

Fig. 1. (a) Damaged steel reinforced concrete hypar-shell at the FH Schweinfurt (Germany), (b) strengthening with TRC, embedding the textile reinforcement (courtesy of S. Weiland).

with five textile layers made of carbon fibre, where the total thickness of the TRC layer was 15 mm. Nine of the 10 slabs include rectangular skylights (Fig. 2). The recalculation of the static load-bearing behaviour of the roof indicated insufficient load-carrying capacity as regards the requirements of the German code for reinforced concrete structures (DIN 1045-1). The construction of a new structure or a truss-support of the roof was precluded by the German authorities for historic preservation. Hence, the strengthening of the structure was essential. In the first step, the surface of the old concrete was sandblasted to remove the weak surface layer, to roughen the surface, and so to guarantee good load transmission between the old concrete and the strengthening TRC layer. Damaged areas of the substrate were removed and the surface re-profiled with a repair mortar. After the surface was pre-wetted, the first layer of fine-grained concrete was applied using a wet-spray method. Eventually, a layer of the textile reinforcement was worked into the fine-grained concrete by slightly pressing and smoothing it with a trowel. This procedure was repeated until reaching the required number of layers. The last textile layer was covered by a layer of fine-grained concrete with a thickness of approximately 3 mm.

TRC can also be used in prefabrication for new construction. Butler et al. [3] described in detail two such examples: a façade panel and a hybrid pipe system with an inner plastic layer. Jesse and Jesse [4] used segments made of TRC for construction of a pedestrian bridge with bondless pre-stressing. Another pedestrian bridge with a record length of 100 m was composed of six large precast TRC elements [5].

1.2. Scope of investigation

The permeability of concrete has an important impact on its durability and correlates primarily with the rate of penetration and the movement of moisture, which may contain aggressive chemicals. In recent years numerous examinations of the permeability of different concretes and cementitious composites in their cracked and uncracked states have been conducted, see e.g. [6–11]. Hoseini et al. [12] summarized in a review the effect of loading type, crack dimension, admixtures, and fibre reinforcement on the permeability of fluids in concrete under stress. This state-of-the-art report on the effect of mechanical loading on permeability presents an account of various test methods which were developed for this purpose. However, only very limited research has been performed on the permeability of TRC [13]. No systematic study is known on this subject to date.

In instances where TRC is used as a material in strengthening or repair, the protection of the existing structural members against the corrosion of concrete and steel reinforcement is an important function of the TRC layer. This function must be considered with an eye to durability in the design of repair and strengthening measures to ensure the effective and reliable use of the new technology. Since the protective function of TRC layers depends directly on their resistance to the transport of fluids and gases into and through the repair material, knowledge and understanding of the mechanisms governing the transport of these media in TRC are required.

Fine crack distribution in the reinforcing TRC layer as shown in Fig. 3 leads one to expect that TRC is less permeable in comparison with cracked ordinary concrete. However, there are numerous cracks which, even though narrow, might affect considerably the transport properties of TRC. Furthermore, textile reinforcement itself might also influence water capillary suction and permeation.

This paper presents the results of an experimental investigation on the effect of multiple cracking of cementitious composites on capillary water absorption as well as water and gas permeability of TRC specimens in both the crack-free and cracked states. The variable parameters in the investigations were the characteristics of the textile reinforcement (materials, fineness, polymer coating).

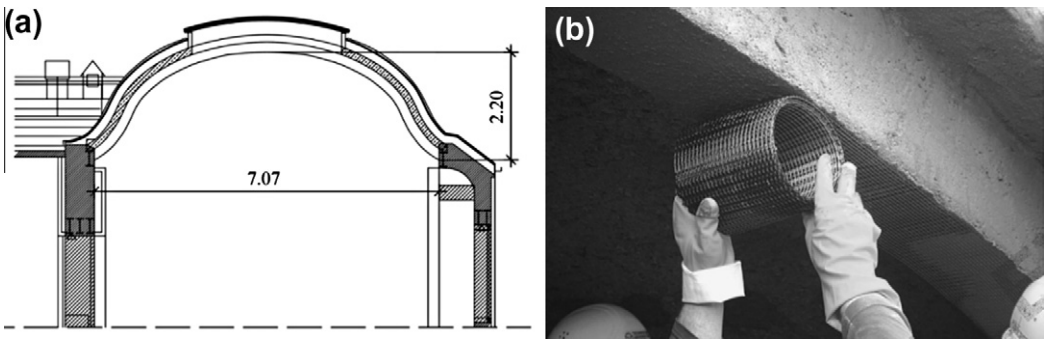

Fig. 2. (a) Cross-sectional drawing of the barrel-shaped roof, (b) placing of the textile reinforcement (courtesy of F. Schladitz).

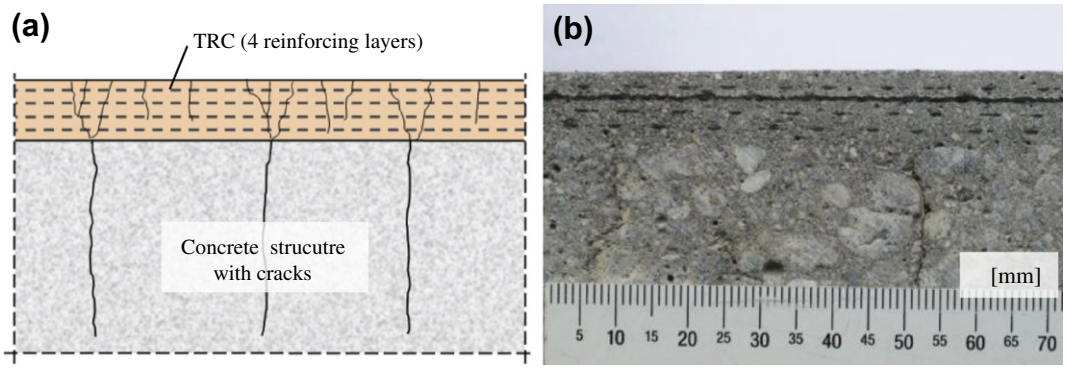

Fig. 3. Schematic view (a) and example (b) of cracked concrete member with TRC with 4 reinforcing layers made of carbon textiles.

The development of a special chamber for in situ permeability testing enabled measurements of water and gas transport properties of cracked TRC at chosen strain levels up to 0.5% under tensile loading. Furthermore, the influence of the self-healing of fine cracks on permeability was investigated.

2. Materials and preparation of specimens

2.1. Fine concrete matrix

The matrix composition used in this study was developed with an eye to the requirements of workability, good bonding to the textile reinforcement, durability, and other considerations [14]. The type of cement chosen and a relatively high content of a pozzolanic addition positively influence the durability of the glass filament yarns and the long-term properties of the matrix-to-yarn interface. Due to this specific matrix composition, a considerable reduction in the pH value of the pore-liquid in the fine concrete was achieved. Furthermore, the voluminous low-strength and alkaline CH phases (portlandite) in the interface were replaced by much more finely structured CSH phases. In this way, high fibre durability and robust performance of the interface over the time were ensured [14].

Table 1 shows the composition of the matrix used for the production of TRC specimens. It consisted of 4 parts by weight of fine sand with a maximum grain size of 1 mm, 3 parts by weight of binder and 1 part by weight of water. The binder was composed of two parts by weight of cement and one part by weight of a pozzolanic addition, a mix of 90% fly ash and 10% silica fume (solid matter). The water to binder ratio was 0.33. A super plasticizer on basis of polycarboxylate ether (PCE) was used as additive.

Table 1
Mix proportions of the TRC matrix.

Material	Mass ratio [-]	Mix proportion [kg/m^3]
CEM III B 32.5N-NW/HS/NA	2.0	550
Fly ash	0.9	248
Micro silica suspension (solid:water = 1:1)	0.2	55
Fine sand 0/1	4.0	1101
Water	0.9	248
Super plasticizer	0.03	8

2.2. Textile reinforcements

Four different types of biaxial textile reinforcements made of alkali-resistant glass (AR glass) and one made of carbon were used as reinforcement for the specimens in this investigation, see Table 2. It should be noted here that from a civil engineering perspective, the fineness of the yarns indicates the degree of reinforcement, i.e. a higher number of filaments in the particular yarn. The reinforcement ratio and the yarns' properties were equal in both directions, i.e. for both warp and weft, cf. Fig. 4. Variable parameters were the fineness of the yarns and the presence or absence of a coating. A polymer coating composed of styrene–butadiene was used to improve the bond between the textile and the surrounding finely grained concrete matrix as well as the bond between the outer and inner filaments in the yarn. Thus, the mechanical performance of TRC increased significantly [15]. The content of the polymer in the yarn was always below 10% by weight.

2.3. Preparation of specimens

Rectangular plates 600 mm long, 100 mm wide, and 14 mm thick were produced with four textile layers. Having straight, plate-shaped specimens is an essential prerequisite for successful transport experiments. It means that the specimens should show no curvature, which mainly occurs due to the difference in shrinkage deformations on the upper and lower surface of the plates. For this reason, two thinner plates, each half of the thickness needed, were cast in separate forms. Subsequently, with the TRC still fresh, one of the forms was turned upside down and placed on the top of another. Both forms were then pressed tightly together, forming the final shape of the plates. The details of this technique are given in Lieboldt et al. [13]. Fig. 5 shows the difference between the

Table 2
Textile reinforcements.

Material		Alkali-resistant glass (AR glass)				Carbon
Yarn fineness	(tex)[a]	1280	2400	1280	2400	800
Filament diameter	(μm)	14	27	14	27	7
Number of filaments per yarn	(–)	3200	1600	3200	1600	12,000
Yarn spacing	(mm)	7.2	7.2	7.2	7.2	7.2
Mass/area	(g/m^2)	364	676	374	707	257
Content of polymer coating	(% by mass)	–	–	2.7	4.6	9.8

[a] tex = g/km.

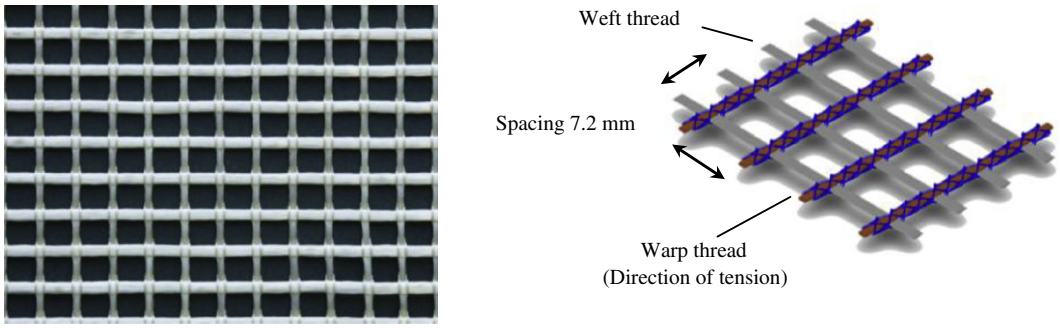

Fig. 4. (a) Sample of a biaxial textile reinforcement made of alkali-resistant glass; (b) schematic view of the textiles used.

Fig. 5. Illustration to the effect of the production technique on the shrinkage of the specimens: a specimen made by casting in two moulds subsequently pressed together (left side), and a specimen cast in one piece (right side).

plates which were cast as one piece, and made of two halves as described above. Due to the unequal shrinkage behaviour at the top side and bottom side of a typical specimen cast in one piece, a considerable degree of curvature develops in such cases, while no such deformations occur for the specimen produced by casting in two moulds subsequently pressed together. The plates were removed from the mould at a concrete age of two days and then stored in water up to an age of 7 days. Then the plates were stored in a climate-controlled room at 20 °C and 65% RH until testing or further preparation.

Before further preparation and testing (water absorption and permeation tests) the specimens were dried at a moderate temperature of 50 °C until no further loss in weight could be observed. Subsequently, the specimens were stored for at least two days in standard climate conditions (20 °C/65% RH) until moisture equilibrium was attained.

3. Experimental investigations and results

3.1. Effect of polymer coating and yarn fineness on water absorption

The textile characteristics, especially the fineness, might exhibit a pronounced influence on the capillary water transport. A simple experiment to find out the effect of textile type in contact with water is the capillary water absorption test. Samples extracted from the TRC plates by sawing were used for such tests at the age of 28 days. A lateral, waterproof seal was applied using a thin layer of wax. The weight before and after sealing, the density, and the exact absorption area were measured and recorded. To determine the effect of textile reinforcement on the capillary water absorption coefficient, prismatic specimens of dimension 100 mm × 150 mm × 14 mm were placed in a water bath so that the unsealed surface of 100 mm × 14 mm was immersed in water (3–4 mm deep). Three specimens were tested for each investigated combination of parameters. The time-dependent change in weight was then measured under standard climatic conditions. The water absorption coefficient w_{24} after 24 h in kg/(m^2 $\sqrt{}$h) was determined for all the specimens using equation:

$$w_{24} = \frac{\Delta W_{24}}{\sqrt{24}} \quad \text{with}: \ \Delta W_{24} = \frac{m_{24} - m_d}{A} \tag{1}$$

where ΔW_{24} is the area-related water absorption, m_{24} is the gross weight of the specimen after 24 h of capillary water absorption in kg; m_d is the dry weight of the specimen weight in kg; and A is the area of the surface immersed in water in m^2.

Fig. 6 shows the water absorption coefficient w_{24} in the direction of the textile layers (parallel to the plate's surface) of the unsealed surface which was immersed in water. The observed results indicate that an increase in the fineness of the yarns leads to an increase in the capillary water absorption. This can be traced to the higher capillary activity of finer yarns. The polymer coating of the textile, on the contrary, leads to a reduction in water absorption due the partial filling of the capillary void volumes with the coating material between individual filaments in the yarn. The reduction in water absorption was between 17% and 23% in comparison with the specimens with uncoated textile, cf. Fig. 6. The lowest water absorption was apparent in the carbon textile, which can be explained by the high polymer content of its coating and the low yarn fineness (small void volume).

3.2. Permeability tests

3.2.1. Sample preparation and test setup

The in situ permeation tests were performed at a specimen age of 56 days or slightly higher. At this age the hydration of binder components was to a large extent completed. The general test set-up followed the approach by Gräf and Grube [16], cf. Fig. 7. A special permeation cell (Fig. 8) made of polymethylmethacrylate (PMMA) was developed for in situ measurements on TRC specimens. The cell was mounted on the specimen and enclosed it tightly. The testing area exposed to gas pressure has a length of 300 mm and a width of 100 mm. The measuring cell, in combination with the built-in specimen, forms two pressure-tight chambers. The seal between the cell and the enclosed specimen was made of a highly elastic sealing material, a special type of silicone. This kind of sealing excluded any significant hindrance of the

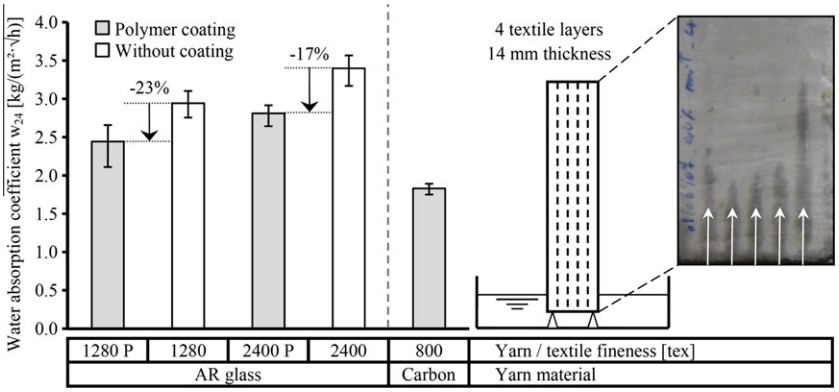

Fig. 6. Influences of yarn fineness and polymer coating on the water absorption coefficient w_{24} (average values, the variations are indicated by brackets); the measurements were performed on uncracked specimen parallel to textile layers.

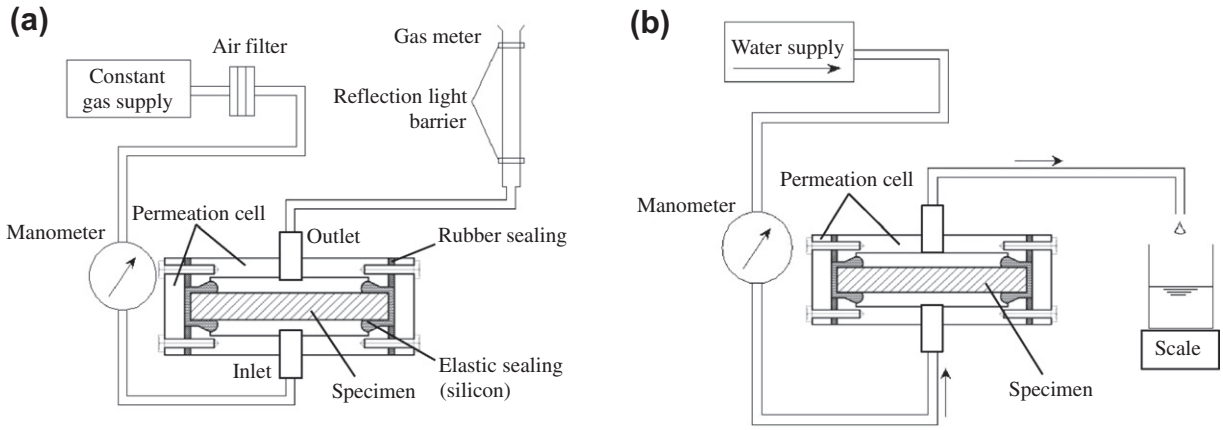

Fig. 7. Schematic view of the test setup for (a) gas permeability, (b) water permeability.

longitudinal deformation of the enclosed TRC specimens by the permeation cell.

The uniaxial tensile load in the in situ measurements was transferred via glued steel plates at the ends of the TRC specimens, cf. Fig 8a. Together, the measuring cell and the steel plates covered the whole main surface areas of specimen. The lateral surfaces outside of the measuring cell (between the steel plates) were sealed with epoxy resin. Thus, a complete sealing of the sample was ensured and the transport of liquids or gases through the textile fabric to the outside at specimen's front ends was excluded. To exclude the presence of leaks in the sealing all specimens were subjected to a leak tests before mounting in the testing machine. The oxygen permeation tests were executed in the state of equilibrium moisture content (cf. Section 2.3) under isothermal conditions in a precisely stabilized laboratory environment (20 °C/65% RH). Oxygen was chosen as the transport medium instead of air in order to exclude the effect of the carbonation processes.

3.2.2. Specific gas permeability coefficient

Oxygen permeation measurements at uncracked and non-loaded TRC specimens were performed as a reference for the in situ gas permeation measurements of cracked samples and for verification of self-healing of fine cracks after the long-term water treatment (cf. Section 3.2.5). The applied gas pressure to the crack-free samples was up to 75 kPa. The recording of permeation data began after a stationary flow condition was established (i.e., linear

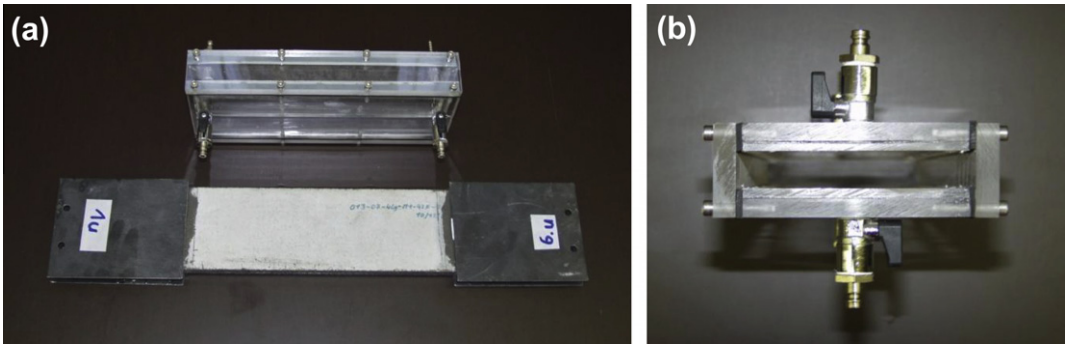

Fig. 8. (a) Permeability cell and specimen, (b) top view of the permeability cell.

pressure distribution through the thickness of the sample). The oxygen flow rate was determined by using a gas meter. This device measures the runtime of a bubble in a measuring burette between two light reflection barriers, cf. Fig. 7a. The specific permeability coefficients of the TRC specimens were calculated using the Hagen–Poiseuille relationship for laminar flow of a compressible fluid in a steady-state condition, given in equation:

$$k = \eta \frac{2 \cdot V \cdot p_0 \cdot h}{A \cdot t \cdot (p^2 - p_a^2)} \quad (2)$$

where k is the permeability coefficient in m^2; η the dynamic viscosity of air in Ns/m^2; V the flow volume in m^3; p_0 the absolute pressure (atmospheric) during the measurements in Pa; h the thickness in m; A the surface area in m^2; t the flow time in s; p the input absolute pressure in Pa, and p_a the outlet absolute pressure (atmospheric pressure) in Pa.

The specific coefficients of oxygen permeability of the TRC plates reinforced with different textiles are given in Table 3. Three specimens were tested for each parameter combination. The determined values in the state ranged between 1.6 and 5.3×10^{-17} m^2. The relatively low permeability values indicate a dense concrete structure and let expect a high durability performance of the crack-free matrix. The permeability coefficients of TRC made of textiles with polymer coating was distinctive lower than those of TRC produced with uncoated textile.

3.2.3. Gas permeation under uniaxial tensile loading (in situ measurements)

The measurements of the oxygen permeability of TRC specimens were performed in situ while the specimens were subjected to uniaxial tension. Since the number of cracks and the summarized crack length on the testing surface of the specimens should be kept constant in order to study the influence of the crack width at different strain levels, the specimens were pre-strained to generate a crack pattern similar to those in practical applications of TRC. For this purpose the specimens were loaded up to a strain level of 0.5% (state IIb, completed crack formation) in the first loading cycle, cf. Fig. 9. Subsequently, the specimen was unloaded and the remaining strain was recorded. Stepwise, the strain level was then increased again up to 0.5%, cf. Fig. 9. In this manner the dependency of the gas permeability on the strain could be determined for a constant summarized crack length and a constant number of cracks, which means that the increase in strain in the second cycle effectuated only the widening of the existing cracks. The number of cracks, crack widths, and the crack pattern were recorded after completion of all testing on each particular specimen. For this purpose the measuring cell was completely removed from the TRC sample. The strain of specimen was controlled by two LVDTs; the strain rate was 0.1%/min.

The oxygen flow rate was measured and recorded at defined strain levels until a steady-state flow rate was established. The test setup allowed determination of the flow rates in a measurement range between 0.01 and 2.5 $dm^3/(s\ m^2)$. Three specimens were tested for each parameter combination. Fig. 10 shows the influence of the imposed tensile strain on the oxygen flow rate (volume flow related to the exposed area) in the case of a gas pressure difference of 3 kPa. A distinctive, non-linear increase in the gas flow rate could be observed with increasing strain, pointing to larger crack openings. The effects of yarn fineness and polymer coating of the textile were clearly recognizable as well. The TRC specimens made with yarn fineness of 2400 tex showed – due to the higher degree

Table 3
Influence of yarn fineness and polymer coating on the specific oxygen permeability coefficient of TRC (perpendicular to textile layers).

Yarn material		AR glass				Carbon
Yarn/textile fineness	(tex)	1280 P[a]	1280	2400 P[a]	2400	800
Specific permeability coefficient k (uncracked material)	($\times 10^{-17}$ m^2)	2.42	4.65	1.64	4.70	2.06
Specific permeability coefficient k (after self-healing)	($\times 10^{-17}$ m^2)	2.72	–	1.82	5.32	2.27

[a] With polymer coating.

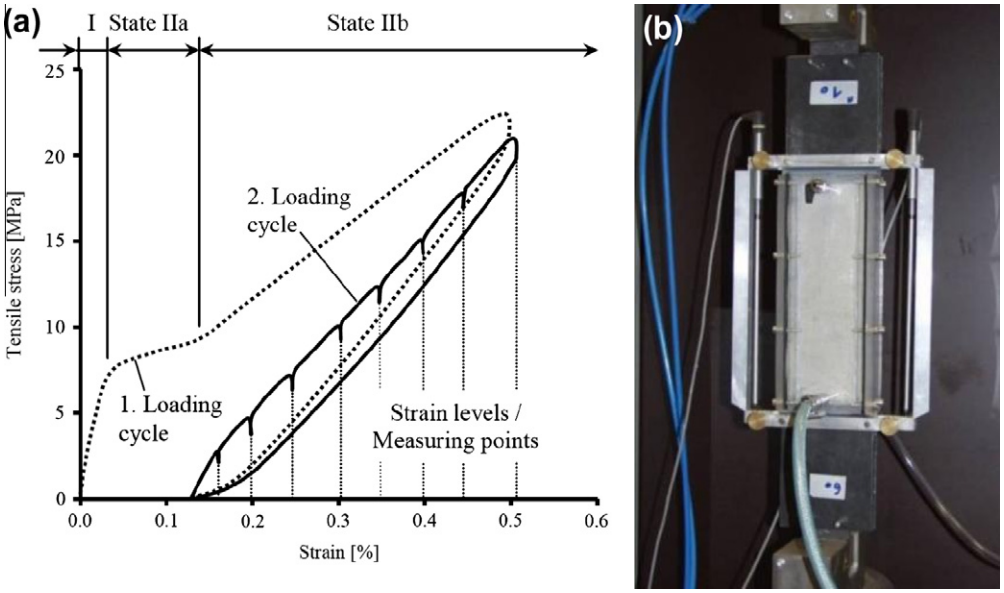

Fig. 9. In-situ permeability measurements under tensile load: (a) loading regime, (b) test setup.

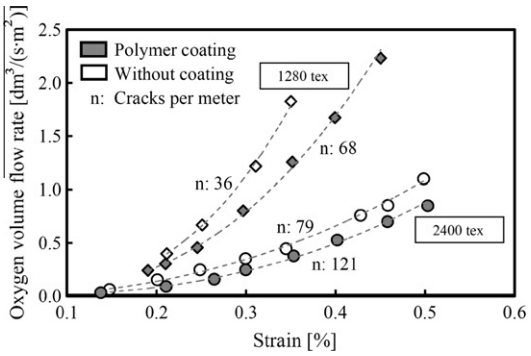

Fig. 10. Effect of induced strain on the oxygen volume flow rate at a pressure difference of 3 kPa for cracked TRC with various yarn qualities.

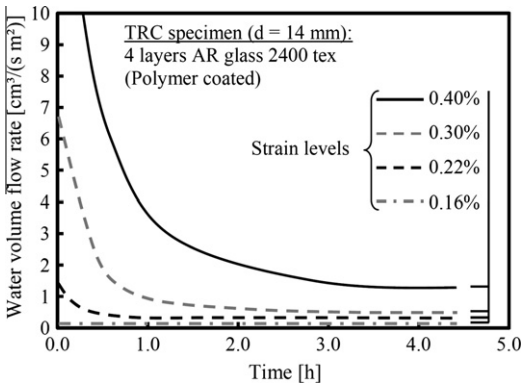

Fig. 11. Time-dependent specific water flow rates of TRC at different strain levels, induced pressure 100 kPa.

of reinforcement – a larger number of finer cracks in comparison to the TRC specimens made with 1280 tex yarns. The polymer coating of the yarns further increased the number of cracks, and herewith the fineness of the crack distribution was enhanced as well. This can be traced back to the coating's improvement of the bond between the individual filaments within the yarn and also between multifilament yarn and the fine concrete matrix, thus enabling a more efficient load transfer. The higher number of cracks was accompanied by a decrease in crack openings. The average crack width in the unloaded state was 65 μm in the case of uncoated textile with a yarn fineness of 1280 tex and 31 μm in the case of TRC with coated yarns. For the specimens made with yarns of fineness 2400 tex, the corresponding average crack widths were 21 μm and 13 μm, respectively.

3.2.4. Water permeation under uniaxial tensile load (in situ)

After completing the gas permeation experiments, a subset of specimens was tested for water permeation. Thus, all samples for water permeation tests possessed the same completed crack patterns (state IIb according to Fig. 9a) as in the oxygen permeation tests. The test setup, including the handling of the permeation cell, was very similar to that used in the gas permeation tests. During the test, the specimen was exposed to constant water pressure on one surface, while the opposite surface was subjected to atmospheric pressure. The water amount passing through the specimen was measured and recorded automatically using a high precision balance.

To determine water permeability the specimens must be fully saturated by water so that the water flow rate through the specimen under given pressure is approximately constant over time. Before applying tension each specimen was saturated with water for at least 24 h. After the specimen was subjected to water pressure in the permeation cell, the saturation of the cement matrix increased further, which led to its swelling, and accordingly, to a partial closure of the cracks. Consequently this also resulted in a decrease in the volume flow rate in time through the specimen. It took at least 2–4 h at each strain level to achieve a quasi-stationary flow state. With increasing applied strain and hence with increasing crack width, a longer time to achieve the steady flow rate was required. Fig. 11 shows the time-dependent flow rates at different strain levels for a sample reinforced with polymer coated textile made of AR glass (yarn fineness 2400 tex).

The effect of the strain on the volume flow rate in the quasi-stationary state is shown in Fig. 12 for TRC made of different textiles. The increase in the transport rate as a function of increasing strain was found to be similar to the material behaviour observed in the oxygen permeability measurements (cf. Fig. 10). The transport rates increased hyper-proportionally at strain levels above 0.2%. The water flow rates were considerably smaller than the oxygen flow rates in spite of the much higher applied pressure, which

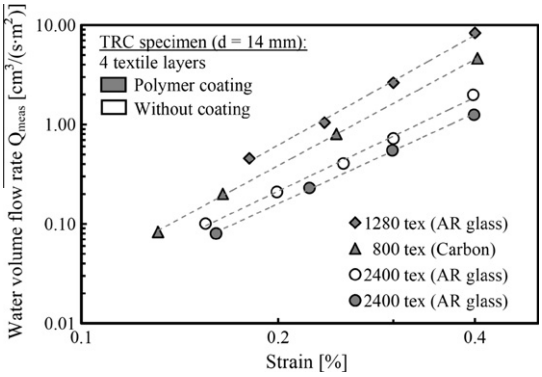

Fig. 12. Effect of the imposed strain level on the specific water flow rate for TRC with different textile reinforcements, induced pressure 100 kPa.

was obviously due to the higher viscosity of water compared to that of oxygen. As expected, the tests on the specimens with finer crack patterns (large number of crack and accordingly smaller crack width for the same stain level) exhibited lower flow rates.

The influence of imposed strain on the permeation of water in cracked TRC prior to self-healing can be predicted by theoretical considerations. A simple, straightforward model based upon Hagen–Poiseuille's Law was used to analyze the water volume flow through a TRC specimen. This law, cf. Eq. (3), describes the fully developed laminar flow of a liquid between two smooth parallel-sided plates. The laminar flow rate increases proportionally with the cube of the crack width (i.e., distance between the parallel plates). However, cracks with smooth parallel-sided surfaces do not occur in concrete. Due to the roughness of the inner crack surfaces, crack branching, the reduction of the crack widths at the vicinity of textile layers, and the reduction of the net crack area at the spots where the textile reinforcement crosses the crack, the measured volume flow rate will be much lower than the estimated one according to Eq. (3).

$$q = \frac{\Delta p \cdot b \cdot w^3}{12 \cdot \eta \cdot d} \tag{3}$$

$$Q_{\text{calc}} = \xi \cdot \frac{\Delta p \cdot b \cdot n \cdot (\varepsilon \cdot l_s)^3}{12 \cdot \eta \cdot d \cdot n^3 \cdot A} \times 10^6 \tag{4}$$

where q is the water flow rate (idealized) (m^3/s); Q_{meas} the measured water flow ($cm^3/(s\,m^2)$); Q_{calc} the calculated water flow ($cm^3/(s\,m^2)$); Δp the water pressure gradient (N/m^2); b the length of crack (m); $b \cdot n$ the summarized crack length (m); w is the crack

width (m); d the thickness of specimen (m); ε the induced strain (–); l_s the length of deformation range (m); n the number of cracks (–); η the viscosity of water (Ns/m^2); A the permeated area (m^2); ξ is the flow coefficient (-).

Further reasons for a decrease in water flow are the reduction of the crack width as a result of advance saturation and swelling of the cement matrix. Thus, Eq. (3) was modified by introducing a flow coefficient ξ and adapted to consider multiple cracking at given strain levels and the geometrical properties of the tested TRC samples, cf. Eq. (4). The coefficient ξ corresponds to the ratio Q_{meas}/Q_{calc}. The average crack width w was expressed by total deformation ($\varepsilon \cdot l_s$) divided by the number of cracks n: $w = \varepsilon \cdot l_s \cdot n^{-1}$. This means that the model assumes that all cracks possesses the same crack geometry (width, length), where elastic strains of the material between the cracks are neglected. These assumptions are certainly a very rough approximation of real conditions. In future work a more comprehensive modelling approach will be developed by the authors. Still, the present model is considered to be a useful first step.

For each of the four specimens tested (each one representing a different TRC), values of the flow coefficient ξ were first determined individually for every measured strain level. No clear dependence of this coefficient on the imposed strain level could be determined in the water permeation test. Subsequently, the flow coefficient ξ was fitted using the method of least squares of the deviations $Q_{meas} - Q_{calc}$ for each specimen using the data obtained at different strain levels. The ξ-values varied between 0.28×10^{-3} and 0.75×10^{-3}. Fig. 13 shows the estimated water volume flow rates Q_{cal} calculated with the fitted ξ-values as a function of the strain level.

The comparison of the measured flow rates Q_{meas} (cf. Fig. 12) and calculated flow rates Q_{calc} (cf. Fig. 13) produced generally good correspondence. However, since the assumptions for the model are rather rough and straightforward, it may not always predict flow values for different strain levels sufficiently well (see values for TRC with the yarn fineness of 1280 tex in Fig. 14). This can be traced back, at least partly, to the fact that with increasing strain the widening of individual cracks differs: some cracks open more widely than other cracks in the same specimen.

3.2.5. Self-healing of cracks

Following the in situ water permeation measurements (third loading cycle), the samples were left in the permeation cell. In order to investigate the effect of self-healing on the transport properties of TRC, further water permeation measurements were carried out in the unloaded, saturated state of specimens at time intervals of 7 days. Fig. 15 shows the time-dependent reduction of the transport rates of samples with different reinforcement

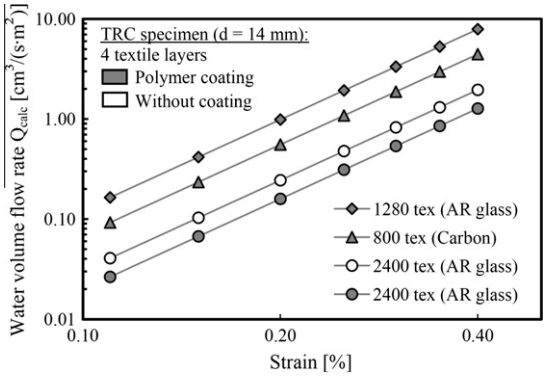

Fig. 13. Calculated strain-dependent specific water flow, pressure 100 kPa.

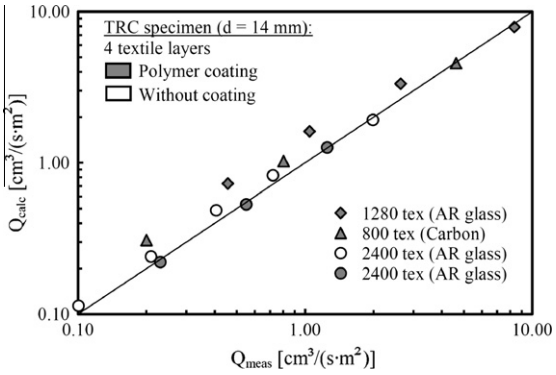

Fig. 14. Relationship between Q_{meas} and $Q_{calc.}$

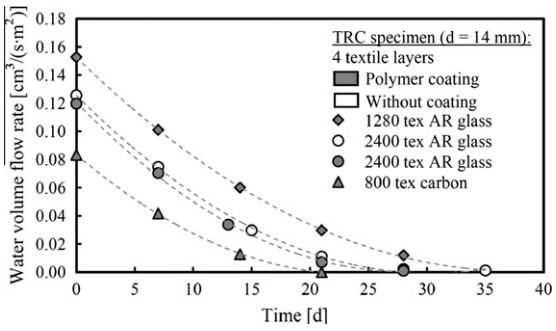

Fig. 15. Time-dependent reduction of the water transport trough cracked TRC in unloaded state.

textiles. After storing the cracked specimens in water for 14 days, the flow rate was reduced to less than 50% of the value obtained on the same specimen before the water storing. No measurable volume flow occurred after continued water exposure of 21–35 days, the particular duration depending on the type of the textile reinforcement used. The samples containing uncoated AR glass yarns with low yarn fineness (1280 tex) needed a longer time until a negligible volume flow was reached, which can be traced back to the initially wider cracks in these specimens. The specimens containing coated carbon textile layers showed the fastest self-healing, which could be expected since they had the finest cracks.

The reduction in the flow rate resulted mainly from the formation of new crystal structures in the fine cracks and additional hydration of the previously non-reacted material as well as from the swelling of cement gel (primarily C–S–H) due to additional water intake. In order to eliminate the influence of swelling, a further oxygen permeability test was performed after water storage of up to 35 days. Since the specimens were dried before the oxygen permeation test, the effect of swelling of the cement matrix could be excluded. The verification should be apparent from the comparison of the oxygen permeability (cf. Section 3.2.2) measured before the first loading cycle (crack-free samples) and after the second loading cycle (cracked samples) with the results of the additional tests on the dried specimens after long-term water storage. Oxygen permeation was reduced to a minimum; the flow rates were similar to the reference measurement data of the crack-free samples before the first loading. Hence, the obvious explanations for the measured decrease in the gas volume flow rate are the self-healing of fine cracks and further hydration of the cement matrix.

Using an Environmental Scanning Electron Microscope (ESEM), additional investigations of cracks before and after exposure to water revealed the formation of new crystal structures which

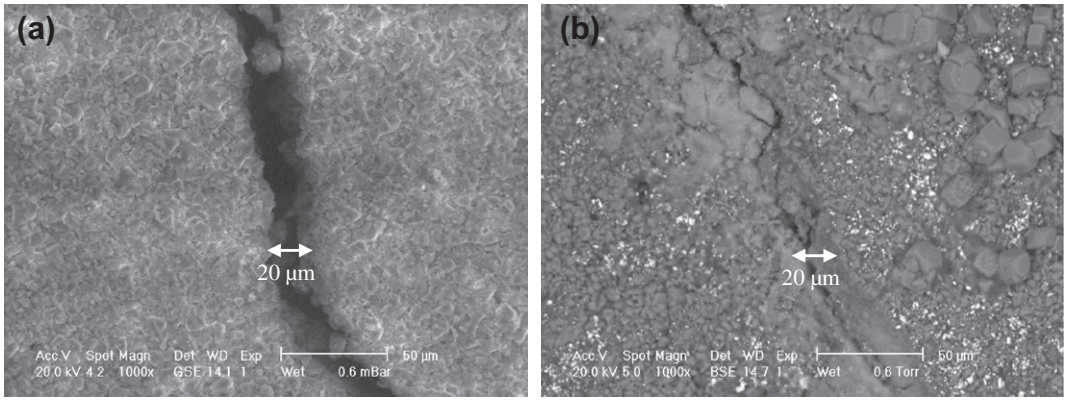

Fig. 16. Self-healing effect: (a) crack before and (b) after water exposure; magnification: 1000×.

closed the cracks to transport, cf. Fig. 16. Fig. 16a shows the original crack with a width of 20 µm before water contact. Fig. 16b illustrates the condition of a similar crack after the water permeability tests with duration of 21–35 days, indeed largely closed by deposits of calcium carbonate (calcite).

4. Summary and conclusions

In applications where TRC is used as a repair and strengthening material, the transport properties of TRC for liquids and gases are of major importance with regard to both the durability of the composite material itself and the protection of the existing structural reinforced concrete members against the corrosion of concrete and steel reinforcement. In this investigation water absorption as well as gas and water permeability tests were performed on specimens made of TRC to estimate the effects of the type of textile, yarn coating, and TRC cracking thereon. The main results can be summarized as follows:

- Measured parallel to the reinforcing textile layers, water absorption of TRC increases with increasing fineness of multifilament yarns and decreases with an increasing amount of polymer used to coat the yarns. Both these observations can be traced back mainly to differences in the capillary system formed in multifilament yarns.
- The oxygen permeability coefficient of the crack-free TRC specimens was clearly influenced by the polymer coating of textile but was only marginally dependent on the fineness of multifilament yarns in the textile. The corresponding permeation coefficients were reduced up to 65% if coated textiles were embedded into the composite instead of uncoated textile.
- Permeation in situ tests on cracked TRC subjected to uniaxial tensile load revealed a pronounced non-linear increase in the transport rates of oxygen and water through the TRC (perpendicular to the composite surface) with increasing strain, which corresponded to larger crack widths. A higher degree of fineness in the textile reinforcement (i.e. a higher degree of reinforcement) as well as the polymer coating of the multifilament yarns led to a larger number of cracks in the TRC specimens at given strain levels, but these cracks were considerably finer. As a result, the permeability for oxygen and water through the TRC made with such reinforcement was lower. This effect was distinctly apparent at strain levels above 0.2%.
- The influence of imposed strain on the permeation of water through cracked TRC could be described by a simple model based upon Hagen–Poiseuille's Law. The model should be refined in future investigations in order to enable a more realistic description of the transport mechanisms in TRC.
- Self-healing of fine cracks in TRC led to a considerable reduction of the transport rates of water and oxygen over time. After a few weeks of storage of the cracked specimens in water, no further measurable volume flow could be observed.

In summary it can be concluded that multiple cracking with relatively small crack widths in comparison to ordinary cracked concrete generally results in the increased resistance of this material to the ingress of fluids and gases. It can be assumed that herewith also the ingress of corrosive substances (e.g. chlorides or sulphates), which often lead to a deterioration of concrete and steel reinforcement, may be considerably reduced. However, further experimental and theoretical investigations are required in order to characterize the long-term behaviour of TRC layers relative to the protective function of this innovative material. This holds true also with respect to the development of a comprehensive model for description of transport properties of TRC.

Acknowledgements

This project was initiated in the Collaborative Research Centre SFB 528 "Textile Reinforcement for Structural Strengthening and Retrofitting" financed by the German Research Foundation (DFG). The authors would like to acknowledge with gratitude the foundation's financial support.

References

[1] Ortlepp R, Weiland S, Curbach M. Restoration of a hypar concrete shell using carbon–fibre textile reinforcement concrete. In: Proceedings of the international conference excellence in concrete construction through innovation, vol. 9–10, London, UK, September 2008. p. 357–64.
[2] Schladitz F, Lorenz E, Jesse F, Curbach M. Strengthening of a barrel-shaped roof using textile reinforced concrete. In: Proceeding of 33rd symposium of the international association for bridge and structural engineering IABSE, September 9–11, Bangkok, Thailand, 2009. p. 416–17 and CD-ROM.
[3] Butler M, Lieboldt M, Mechtcherine V. Application of Textile-Reinforced Concrete (TRC) for structural strengthening and in prefabrication. In: advances in cement-based materials, London: Taylor & Francis Group, 2010. p. 127–36.
[4] Jesse D, Jesse F. Textile reinforced concrete for lightweight segmental bridges with post-tensioning. In: Proceedings of 3rd international fib congress, May 29–June 2, Washington, DC, USA, 2010. Paper 154 (DVD-Rom).
[5] Hegger J, Kulas C, Goralski C. Elegant foot-bridge of textile-reinforced concrete – design and construction. Concrete plant + precast technology, vol. 76, no. 2. BFT International, 2010. p. 60–1.
[6] Wang K, Jansen DC, Shah SP. Permeability study of cracked concrete. Cem Concr Res 1997;27(3):381–93.
[7] Lawler JS, Zampini D, Shah SP. Permeability of cracked hybrid fiber-reinforced mortar under load. ACI Mater J 2002;99(4):379–85.
[8] Gerard B, Breysse D, Ammouche A, Houdusse O, Didry O. Cracking and permeability of concrete under tension. Mater Struct 1996;29(3):141–51.
[9] Edvardsen C. Water permeability and autogenous healing of cracks in concrete. ACI Mater J 1999;96(4):448–54.

[10] Reinhardt HW, Jooss M. Permeability and self-healing of cracked concrete as a function of temperature and crack width. Cem Concr Res 2003;33(7):981–5.
[11] Lepech MD, Li VC. Water permeability of engineered cementitious composites. Cem Concr Compos 2009;31(10):744–53.
[12] Hoseini M, Bindiganavile V, Banthia N. The effect of mechanical stress on permeability of concrete: a review. Cem Concr Compos 2009;31(4):213–20.
[13] Lieboldt M, Barhum R, Mechtcherine V. Effect of cracking on transport of water and gases in textile reinforced concrete. In: Proceedings of 8th international conference on creep, shrinkage and durability mechanics of concrete and concrete structures – CONCREEP-8, September 30–October 2, Ise-Shima, Japan, 2008. p. 199–205.
[14] Butler M, Mechtcherine V, Hempel S. Experimental investigations on the durability of fibre–matrix interfaces in textile-reinforced concrete. Cem Concr Compos 2009;31(4):221–31.
[15] Butler M, Hempel R, Schorn H. Bond behaviour of polymer impregnated AR-Glass textile reinforcement in concrete. In: Proceedings of the international symposium polymers in concrete, April 2–4, Guimaraes, Portugal, 2006. p. 173–83.
[16] Gräf H, Grube H. Experimental testing method of water and gas permeability of mortar and concrete: Part 1. Beton 1986;36(5):184–7 [in German].